Journal of Nuclear Materials 385 (2009) 461–466

Contents lists available at ScienceDirect

Journal of Nuclear Materials

journal homepage: www.elsevier.com/locate/jnucmat

Helium solubility and behaviour in uranium dioxide

E. Maugeri [a,*], T. Wiss [a], J.-P. Hiernaut [a], K. Desai [b], C. Thiriet [a,1], V.V. Rondinella [a], J.-Y. Colle [a], R.J.M. Konings [a]

[a] European Commission, Joint Research Centre, Institute for Transuranium Elements, P.O. Box 2340, 76125 Karlsruhe, Germany
[b] Dept. of Materials, Imperial College London, South Kensington Campus, London SW7 2AZ, United Kingdom

ARTICLE INFO

PACS:
61.82.Ms
66.30.je
67.25.−k
68.43.Vx

ABSTRACT

A set of devices was developed in order to infuse UO_2 disks with helium, at high temperature and pressure, to measure the helium infused quantity and from these data to calculate the helium solubility in the UO_2 matrix. Samples of UO_2 single crystal and UO_2 polycrystal were infused at a temperature of 1473 and 1743 K in a helium atmosphere ranging between 50 and 100 MPa. These samples were then annealed and the helium released was measured with a mass spectrometer. From the obtained spectra it was possible to give an interpretation of the helium release mechanism and to calculate its solubility in the UO_2 lattice in these specific thermodynamic conditions. Additionally to the helium solubility measurement from infused samples, a 37 years old sample of $^{238}PuO_2$, retrieved from an old ^{242}Cm radioisotope thermoelectric generator (RTG), containing radiogenic helium, was also measured to widen perspectives of this kind of measurements to damaged sample more representative of spent fuel.

1. Introduction

This study aims to understand and to forecast the physical–chemical state of the spent nuclear (typically UO_2) fuel after a long time of storage. The spent nuclear fuel is not in thermodynamical equilibrium because it contains radioactive elements that, because of their decay, cause continuous modification of its physico-chemical properties. After several centuries, the residual activity will be mostly due to α-decaying actinides that will generate large quantities of helium in the spent fuel matrix. Another consequence of α-decay is radiation damage mostly due to recoil nuclei, causing the formation of point defects that can grow into three-dimensional defects such as dislocations. The accumulation of helium linked to alpha-damage could result in precipitation of bubbles at the grain boundaries, which could eventually cause loss of grain cohesion, thus reducing the spent fuel pellet to powder. Subsequent accidental contact with water would be greatly affected by the change of its physical state, namely by the dramatic increase of the surface area exposed to water, and potentially enhanced by radiolysis. For these reasons it is important to understand the helium behaviour in the spent fuel. In particular it is necessary to measure its solubility and to determine its location in the UO_2 lattice. The knowledge of the helium solubility will allow us to assess the maximum quantity that can be accommodated in the lattice. Solubility values have been reported previously (e.g. Rufeh et al. [1]). Within the experimental conditions used in the past [1–3] (maximum 10 MPa) it was found that the solubility follows Henry's law. This paper reports on the solubility measured on UO_2 samples infused with helium at higher pressure (between 50 and 100 Pa) and at higher temperature (up to 1743 K). A set of devices has been designed for this purpose; the first consists of a device to infuse the UO_2 sample with helium at high pressure (up to 200 MPa) at high temperature (up to 1800 K), the second is a high temperature Knudsen cell furnace coupled to a mass spectrometer to anneal the sample to release the infused helium and measure its release profile as a function of the temperature. To quantify the released helium a third device collects the released gas and measures it by a mass spectrometer. The first results on solubility and the technical development are presented, together with helium solubility determined from the helium release experiments of infused samples. The helium behaviour in different systems, from the most basic (UO_2 infused with helium) to the more complex (polycrystal UO_2 and PuO_2), will be described based on helium thermal desorption.

2. Experimental

The experimental procedure employed in this study is presented schematically in Fig. 1.

The Helium Infusion Device (HEIDI) aims at infusing a UO_2 sample with helium by heating the sample with a laser (continuous wave 5 kW Nd:YAG laser at 1064 nm) at high temperature under high pressure of helium. It consists of a 200 MPa autoclave (A in Fig. 1) in which is placed a crucible holding the UO_2 sample. It is equipped with a sapphire window placed parallel to the sample

* Corresponding author. Tel.: +49 7247 951 149; fax: +49 7247 951 99 149.
E-mail address: emilio.maugeri@ec.europa.eu (E. Maugeri).
[1] Present address: Atomic Energy of Canada Limited, Chalk River Laboratories, Chalk River Ontario, Canada KOJ 1JO.

0022-3115/$ - see front matter © 2008 Elsevier B.V. All rights reserved.
doi:10.1016/j.jnucmat.2008.12.033

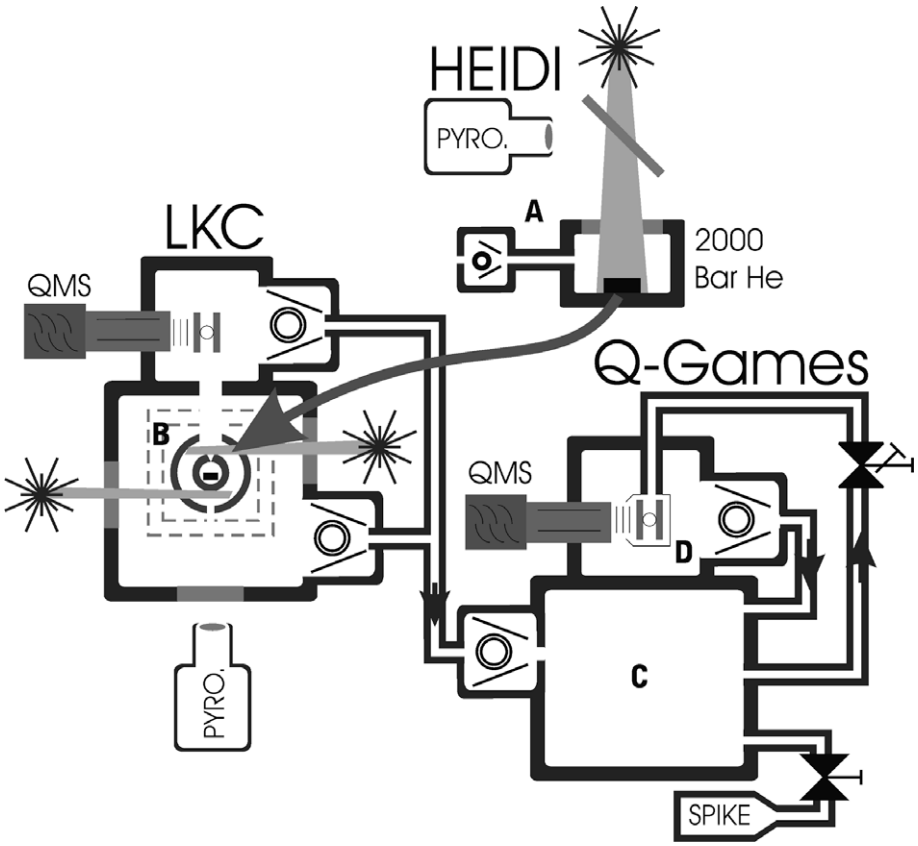

Fig. 1. Scheme of the experimental set up developed to quantitatively measure the infused helium in a UO_2 sample at high pressure (up to 200 MPa) and high temperature (up to 1800 K), comprising: (A) helium infusion device (HEIDI); (B) Laser Knudsen Cell (LKC); and (C) quantitative gas measurements (Q-GAMES).

surface. In order to have a homogeneous helium profile, it is necessary to have a uniform radial and axial thermal gradient in all the sample. Therefore, a laser beam coming from a 600 μm light guide, is focused on the sample and irradiates it perpendicularly to its surface. The laser spot size has a diameter slightly larger than the sample to avoid radial temperature gradient. The sample is placed in a UO_2 crucible since the use of the same sample material reduces temperature gradients between the sample and the crucible itself. The sample has a diameter of 3 mm and it is thin enough (300 μm) to avoid axial temperature gradient. The sample temperature is measured by a pyrometer perpendicularly to its surface, in the same optical axe than the laser beam, via a dichroic mirror.

Next a Laser Knudsen Cell (LKC) [4], is used to release the helium from the UO_2 sample previously infused by annealing and to measure the helium release profile as a function of the temperature. It is a laser heated furnace (B in Fig. 1) consisting of a spherical Knudsen cell placed in the centre of a spherical susceptor acting almost like a black body cavity in which laser light (up to 5 kW) is injected. A horizontal black body hole is drilled in the cell to measure the temperature with a pyrometer. This system is coupled to a mass spectrometer. Finally the quantitative gas measurements (Q-GAMES) device is used to make quantitative measurement of the gases released from a sample during the annealing in the LKC. It consists of a sample chamber (C in Fig. 1), evacuated prior to the experiments at a pressure of 10^{-4} Pa, where the exhaust gases (containing the released helium) coming from LKC are collected. This chamber is directly connected, by a leak valve, to a second chamber (mass spectrometer chamber, D), with a background pressure of 10^{-8} Pa, in which a QMS (quadrupole mass spectrometer) measured the sampled gas. To allow better sensitivity and to avoid losses of signal by pumping, the gas pumped in the mass spectrometer chamber is fed back into the sample chamber. To make gas quantitative measurements, a spike system allows introduction of a well defined quantity of spike gas to the sample chamber after all released gas has been collected from the LKC and by comparing the signal before and after the introduction of the spike, it is possible to quantify helium released from the infused sample. The dynamic range of measurement is between 10^{-12} and 10^{-5} mol with a relative error below 2%.

3. Samples

The reported experiments were carried out with three different kinds of materials:

(a) Two disks of UO_2 single crystal infused with helium.
(b) Four UO_2 polycrystal disks, cut from the same pellet fabricated by a sol-gel technique [5–7], also infused with helium.
(c) A 37 years old sample of $^{238}PuO_2$, retrieved from an old ^{242}Cm radioisotope thermoelectric generator (RTG), containing radiogenic helium, in the form of powder of about 1 μm grains mostly agglomerated (up to 500 μm);the last sample was included to broaden the perspective of this kind of measurement to radiation damaged samples more representative of spent fuel.

3.1. UO_2 single crystals

Finite element quantity techniques Flex PDE 4.0.0.code [8] was used to calculate that it is possible to obtain a homogeneous

temperature distribution in all the UO_2 sample volume, infusing disks of 0.3 mm thickness and 3 mm diameter. To avoid having samples with different characteristics and thus biased results, disks were cut from the same UO_2 single crystal. To remove defects due to the cutting and to guarantee the correct stoichiometric, the two disks were annealed for 4 h at 1400 K in argon atmosphere with 4% hydrogen. The two samples were separately infused in HEIDI, with a helium pressure of 100 MPa, for 1 h, at 1523 and 1743 K respectively. After, the infusion the samples were placed into the LKC, where they were annealed with the following temperature program: 50 K min^{-1} temperature ramp to1873 K with a plateau of 5 min at 1773 K. The released gas was collected, measured and compared with the signal of a known spike of ^4He, in the Q-GAMES.

3.2. UO_2 polycrystals

Four disks of UO_2 polycrystal of 0.3 mm thickness and 3 mm diameter, cut from the same pellet, were annealed in argon atmosphere with 4% of hydrogen like the single crystal samples. The first two samples were infused at a helium pressure of 100 MPa, at 1473 K for 1 h, while the last two were infused at a helium pressure of 50 MPa, at 1473 K for 2 h. After infusion, the samples were placed into the LKC, where they were annealed with the following temperature program: temperature ramp 50 K min^{-1} to 2200 K. The released gas was collected, measured and compared with the signal of a known spike of ^4He, in the Q-GAMES.

3.3. ^{238}Plutonium dioxide

Study on helium release of $^{238}PuO_2$, taken from an old ^{242}Cm radioisotope thermoelectric generator, were carried out in order to expand the perspectives of this kind of measurements to damaged sample more representative of spent fuel.

The $^{238}PuO_2$ powder constituted of grains of about 1 μm, mostly agglomerated (~500 μm agglomerates) with an activity estimated of $4.5–5 \times 10^{11}$ Bq·g^{-1}, was kept in a sealed container for about 37 years. The atmosphere in the container was mostly composed of the radiogenic helium not retained in the grains due to the larger range of the alpha-particles than grain size.

A fraction of 10.8 mg of this $^{238}PuO_2$ was annealed in an active Knudsen cell. The cell was made of tungsten and operated under high vacuum (10^{-4} Pa) up to 2800 K.

The sample was annealed with the following temperature program: temperature ramp 50 K/min to 2200 K. The released gas was collected, measured and compared with the signal of a known spike of helium-4, in the Q-GAMES.

4. Results

4.1. Helium release from UO_2 single crystal

Fig. 2 shows the helium released from the single crystal sample, as a function of time, using the LKC mass spectrometer (hereafter denominated curve A) and Q-GAMES mass spectrometer (hereafter denominated curve B). Curve A is a derivative signal while the curve B is an integrated one. From curve A we can deduce information on the release mechanism. Two characteristic temperature ranges assigned to two different release mechanisms can be distinguished. At the lowest temperature, around 600 K, the observed peak is attributed to helium adsorbed on the UO_2 sample surface [1,2]. Integrating this quantity of adsorbed helium shows that it represents a fraction less than 7.5% of the total quantity desorbed and it is not taken into account in the calculation of the helium solubility. The release of helium that occurs around 850 K is likely due to helium depletion of the surface. In this first stage, at relatively low temperature, only the helium near the surface is released. The depletion of this volume, no deeper then a few μm, contributes to the driving force for the bulk helium release. An analogue phenomenon was observed by Martin et al. [9,10] at the UO_2 grain boundary, during an annealing experiment performed on ^3He-implanted samples.

In the region of 1200 K the main release occurs, attributed to helium located in a stable lattice position, likely octahedral interstitial sites, i.e. the cavities in the middle of the oxygen cubes of the UO_2 structure, as shown as *ab initio* computational studies [11–13]. This result is confirmed by experimental work of Garrido et al. [14], performed by the RBS-channelling technique combined with nuclear reaction analysis, which demonstrates that the preferential lattice position of implanted helium atoms into UO_2 single

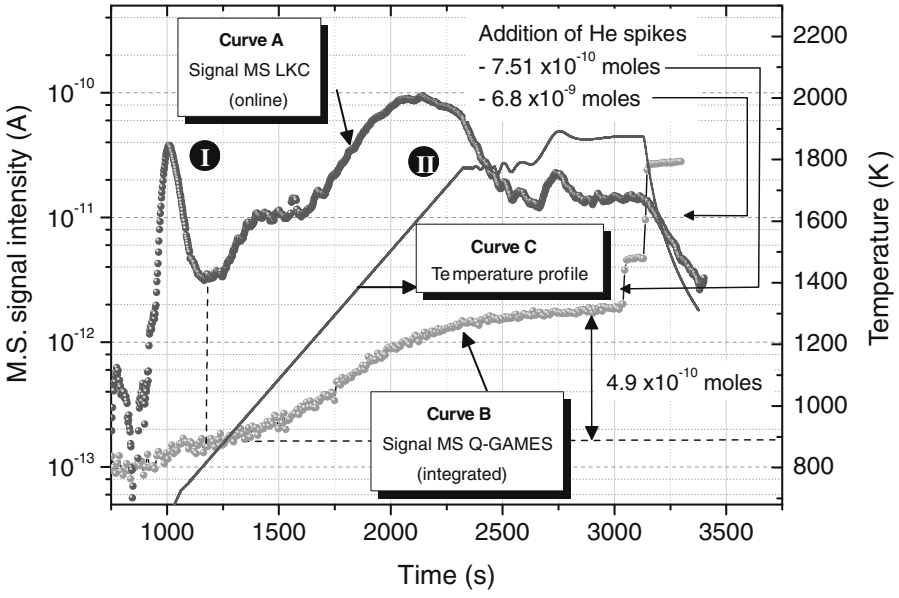

Fig. 2. M.S. signal of the helium released from a UO_2 single crystal sample, infused with a helium pressure of 100 MPa, for 1 h, at 1523 K and recorded online by the LKC mass spectrometer (curve A). The integrated signal of the helium released in the same experiment, measured by the Q-GAMES mass spectrometer is shown, curve B. The curve C shows the annealing temperature profile as a function of time.

crystal is the octahedral site. From these positions helium atoms diffuse to the surface via atomic diffusion. The last peak, corresponding to 5% of the total release, corresponds to the release of the remaining helium due to a temperature increase. From curve B the quantity of helium infused was calculated as $(4.9 \pm 0.1) \times 10^{-10}$ mol helium coming from $2.138 \times 10^{-2} \pm 2 \times 10^{-5}$ grams of UO_2 a single crystal. Dividing the quantity of helium released by the weight of the sample, the helium solubility was calculated to be $2.29 \times 10^{-8} \pm 4 \times 10^{-10}$ mol g^{-1} or $5.13 \times 10^{-4} \pm 10^{-5}$ cm^3 g^{-1} at 1523 K and 10^8 Pa.

4.2. Helium release from UO_2 polycrystal

Fig. 3 shows the release profile of one of the two samples infused at 50 MPa, 1473 K for 2 h (the release from the second sample was exactly identical). Two main release stages were attributed to the profile: the first starts at 1500 K and the second at a higher temperature, although the two mechanisms overlap around 1800 K. The first release is attributed to the helium dissolved in the lattice diffusing to the sample surface through grain boundaries. During this diffusion part of the helium is trapped in intragranular pores of the polycrystal, where infused helium is already located. The helium accumulated in intragranular pores is released, through grain boundaries or through tunnels formed at the grain boundaries, in the second release stage, as also observed by El-Genk et al. in $^{238}PuO_2$ [15]. The third process, which occurs on the top of the two others, is characterized by a series of burst releases. Fig. 3 shows this phenomenon starts at about 1700 K and can be attributed to intergranular pores connections [15–20]. The 'apparent solubility' (which is the solubility calculated considering only the He located in the UO_2 lattice, in the grain boundaries and in the pores) measured is $2.21 \times 10^{-7} \pm 4 \times 10^{-9}$ mol g^{-1} ($4.9 \times 10^{-3} \pm 10^{-5}$ ml g^{-1}) which is 9 times that measured in the single crystal.

A second set of two polycrystal samples was infused at 1523 K, at 100 MPa for 1 h. From the Q-GAMES mass spectrometer spectrum of one of the two samples, an apparent solubility of helium of $(3.6 \pm 0.1) \times 10^{-6}$ mol g^{-1} ($8.1 \times 10^{-2} \pm 10^{-4}$ ml g^{-1}) was measured that is 150 times that measured in the single crystal in the same conditions of temperature, pressure and infusion time. Also in this case the measured helium quantity in the two samples was similar.

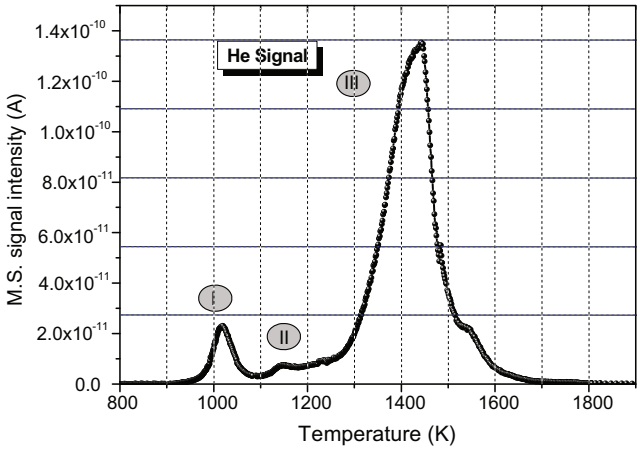

Fig. 4. Derivate signal of the helium released from a 37 years old $^{238}PuO_2$ powder sample, constituted of 1 μm grains, annealed in Knudsen cell and recorded by the Q-GAMES mass spectrometer.

Comparing the two sets of experiments reveals that doubling the pressure (from 50 to 100 MPa), although reducing the infusion time as a factor of 2 (from 2 to 1 h) increases the apparent solubility 16 times. This highlights the important role of the pressure in the infusion process for achieving saturation of the allowed lattice position by the helium atoms.

4.3. Aged ^{238}plutonium dioxide

Fig. 4 reveals that the helium release in the $^{238}PuO_2$ sample starts at 950 K and takes place in three steps. The first release (950–1100 K) is attributed to the helium adsorbed on the surface. At 1150 K a second release is attributed to the helium trapped in pores between the agglomerated grains. This fraction is low and its contribution to the total release is negligible. Between 1150

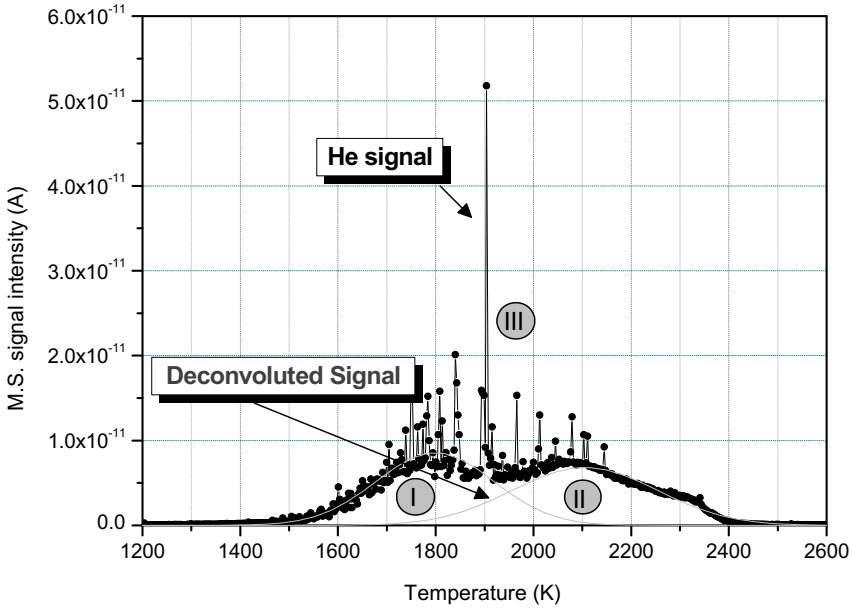

Fig. 3. Helium release curves from a UO_2 polycrystal sample, infused with a pressure of 50 MPa, for 2 h at 1473 K and recorded online by the LKC mass spectrometer, showing three different release mechanisms.

and 1600 K is the main release peak due to release of the helium located in the grains, probably precipitated in tiny bubbles, which diffuses, via grain boundaries, to the surface [21].

The helium quantity measured, $2.43 \times 10^{-7} \pm 5 \times 10^{-9}$ mol, represents only about 3% of the helium generated during the storage, corresponding to an 'apparent solubility' of $2.85 \times 10^{-5} \pm 5 \times 10^{-7}$ mol g^{-1}, which is 1000 times more than the solubility measured for a UO_2 single crystal infused at 1473 K, 100 MPa for 1 h.

5. Discussion

The data on helium solubility obtained in those experiments were compared to data published by Rufeh et al. [1], Sung [2] and Bostrom [3] previously. Based on the release curves from those experiments (see Figs. 2 and 3) and on the influence of the infusion parameters like pressure and infusion time we interpret the obtained solubility values, estimating whether saturation was achieved or not. Rufeh's [1] and Sung's [2] data are plotted in Fig. 5. As stated in their work, helium solubility follows Henry's law and their data are extrapolated accordingly to the pressure values of our experiments. Rufeh et al. [1] infused 4 μm average size particles of UO_2 in a helium atmosphere of 5 and 10 MPa at 1473 and 1573 K, respectively. To measure the helium infused, the samples were melted and the helium released was measured with a mass spectrometer. To avoid measuring the helium trapped in the open pores, the samples were kept under vacuum for two months at room temperature; moreover to remove the helium likely adsorbed on the surface the samples were annealed at 573 K for several hours.

In his work, Sung [2] infused UO_2 particles with an average diameter of about 10 μm at two temperatures: 1473 K and 1623 K and at three pressures: 4.83, 6.89 and 8.96 MPa, respectively. To minimize the phenomena of sintering of the particles during the annealing (phenomena that could cause the adsorption of larger quantities of helium leading to an overestimation of the solubility), the particles were placed between two platinum foils. To remove the helium likely adsorbed on the surface the samples were annealed at 373–473 K for 24 h in a vacuum of 10^{-4} Pa. The samples were dissolved in nitric acid in order to release the helium infused.

Additionally, Bostrom's [3] results were also considered. He infused 0.088 μm particles at 973 K in 0.1 MPa atmosphere of helium for 4 h and 0.16 μm UO_2 particles at 1073 K in 0.1 MPa atmosphere of helium for 6 h.

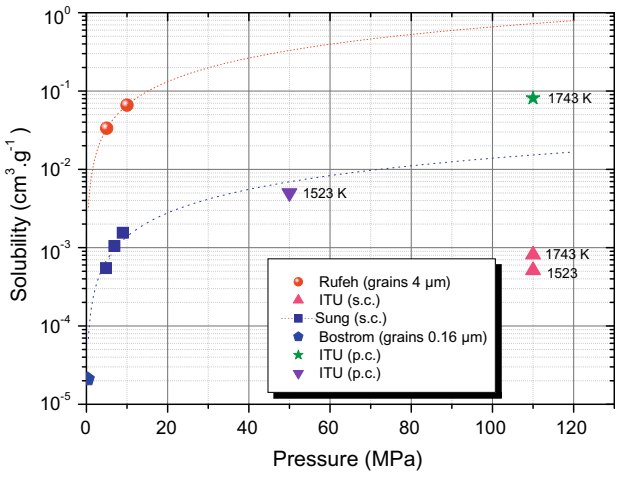

Fig. 5. Summary of the helium solubility in UO_2 single crystal measured by Rufeh, Sung and Bostrom, respectively, and the helium solubility in UO_2 single and polycrystal measured in the present work.

Fig. 5 indicates that both solubilities measured by Rufeh and Bostrom (extrapolating the data at high pressure) are two orders of magnitude higher than that measured by Sung for the same thermodynamic conditions (1473 K and 1–5 MPa) and about three orders of magnitude higher than that measured in this study for a UO_2 single crystal, infused at 1523 K and 100 MPa. This overestimation could be attributed to the fact that both Rufeh and Bostrom used very small particles of 4 μm average size and that some sintering occurred resulting in helium trapping in pores. This phenomenon was avoided by Sung by placing the particles between two platinum foils during the annealing. Moreover, Rufeh used a crushed polycrystal sample and, although the particles were very small, it is possible that some helium has been retained in remaining grain boundaries. This interpretation, although difficult to quantify, can be deduced from the 'apparent solubility' we have measured for a polycrystal infused at 1743 K under 100 MPa atmosphere of helium. This value is between Sung and Rufeh's values extrapolated at 100 MPa. In this case the release has two contributions; one due to the helium coming from the grain and one due to the helium coming from the grain boundaries or from pores.

The difference between the helium solubility values we measured for the UO_2 single crystal and the one extrapolated at the same pressure from Sung's data, using Henry's law, can have various origins, such insufficient infusion time in our experiments (in Sung's experiment [2] helium saturation was achieved after ~24 h), closed porosity in the samples of Sung, systematic analytical differences.

Experiments are ongoing to determine these phenomena. In the case of spent fuel storage, the thermodynamic solubility might be surpassed because of the formation of radiogenic helium. In this case, and because of associated alpha-radiation damage, the helium behaviour might diverge from that observed even in the infused polycrystals. To this respect, an old $^{238}PuO_2$ sample was investigated by helium thermal desorption. The quantity of helium that was retained in the matrix was about 1000 times greater than in a UO_2 single crystal. The large difference between these two data is due to the precipitation of helium in tiny bubbles in the $^{238}PuO_2$ sample as has been observed in Transmission Electron Microscope measurements.

The helium release profile in the $^{238}PuO_2$ can be divided in three mechanisms: the first is due to helium adsorbed on the surface; the second one is due to the helium trapped between the agglomerated grains, this quantity is negligible and the mean release is due to the helium located in the grain, mostly precipitated in bubbles. The helium release profile could be interpreted in term of mechanisms associated with helium migration. The release mechanism of helium in UO_2 single crystal is mainly due to the atomic diffusion instead in the polycrystal this mechanism is marginal and it is mostly due to the diffusion via grain boundaries.

6. Summary

The helium solubility in UO_2 has been measured by using an innovative set of devices, for the infusion on one hand, and for the quantitative measurement of the thermally desorbed helium on the other hand. The accuracy of the method was proved by the congruent results obtained measuring the helium solubility of two sets of UO_2 polycrystal infused in different condition of pressure and infusion time.

The first results of helium solubility in UO_2 single crystal, infused at 1523 K and 100 MPa, obtained was: $5.1 \times 10^{-4} \pm 10^{-5}$ cm^3 g^{-1}.The solubility of helium measured in two sets of polycrystal samples, infused at 1523 K and 50 MPa for 2 h and at

the same temperature but at 100 MPa for 1 h, is respectively 9 and 160 time more the helium solubility measured in the single crystal. This clear difference is attributed to the presence of grain boundaries and pores in the polycrystal. A comparison between the data obtained in this work with those published previously by Rufeh et al. [1] and by Sung [2], leads to the conclusion that helium saturation could be not yet been reached. Experiments are ongoing to determine this infusion time.

Additionally studies were carried out on helium release profile analysis from a $^{238}PuO_2$ specimen. This sample having cumulated alpha-damage is more representative of spent fuel after several centuries of storage. The obtained results show the different helium behaviour in comparison to the infused samples, attributed to the evolution of the microstructure like the formation of helium bubbles or of extended defects [21].

Experiments are planned to determine the influence of different parameter: infusion temperature, infusion helium pressure, time, effects of the grain size in different polycrystalline sample on the He 'apparent' solubility in UO_2. The subsequent step will be the characterization of 'helium infused' specimens to determine the location of He in the UO_2 lattice e.g. with RBS-C.

Acknowledgements

The authors are thankful to F. Capone for the development of the Laser oven and Q-GAMEs and to Dr D. Manara, U. Zweigner and L. Vlahovic for their support in the development of the infusion device. Thanks are also due to G. Pagliosa for helping in the preparation of the samples and Dr D. Staicu for performing the thermal profile calculations.

References

[1] F. Rufeh, D.R. Olander, T.H. Pigford, Nucl. Sci. Eng. 23 (1965) 335.
[2] P. Sung, Equilibrium solubility and diffusivity in single-crystal uranium oxide, PhD thesis, University of Washington, 1967.
[3] W.A. Bostrom, in: Proceedings of the Second United Nations International Conference on Peaceful Uses of Atomic Energy, Geneva, 1958, p. 569.
[4] J.-Y. Colle, F. Capone, J. Sci. Instrum. 79 (2008) (published online).
[5] P.A. Haas, F.G. Kitts, H. Beutler, Chem. Eng. Prog. Symp. 63 (1967) 16.
[6] R. Forthmann, G. Blass, J. Nucl. Mater. 64 (1977) 275.
[7] H. Lahr, Kerntechnick 19 (1977) 159.
[8] Finite elements code Flex PDE, www.floxpdf.com.
[9] G. Martin, P. Desgardin, P. Garcia, T. Sauvage, G. Carlot, H. Khodja, M.F. Barthe, Mater. Res. Symp. Proc., 2007, p. 71.
[10] G. Martin, P. Desgardin, T. Sauvage, P. Garcia, G. Carlot, H. Khodja, M.F. Barthe, Nucl. Instrum. Meth. Phys. Res. Sect. B 249 (2006) 509.
[11] J.-P. Crocombette, J. Nucl. Mater. 305 (2002) 29.
[12] R.W. Grimes, Philos. Trans. Royal Soc. London 335 (1991) 609.
[13] M. Freyss, N. Vergnet, T. Petit, J. Nucl. Mater. 352 (2006) 144.
[14] F. Garrido, L. Nowicki, G. Sattonnay, T. Sauvage, L. Thome, Nucl. Instrum. Meth. Phys. Res. Sect. B 219&220 (2004) 196.
[15] El-Genk, J. Nucl. Mater., vol. 280, 2000, p. 1.
[16] J.A. Turnbull, C.A. Friskney, J. Nucl. Mater. 71 (1978) 238.
[17] C.A. Friskney, J.A. Turnbull, J. Nucl. Mater. 79 (1979) 184.
[18] D.R. Olander, Fundamental aspects of nuclear reactor fuel elements, US ERDA Technical Information Centre, Energy Research and Development Administration Report TID-26711-P1, Springfield, Virginia, 1976.
[19] R.N.R. Mulford, B.A. Mueller, Los Alamos Scientific Laboratory Report LA-5215, 1973.
[20] B.A. Mueller, D.D. Rohr, R.N.R. Mulford, Los Alamos Scientific Laboratory Report LA-5524, 1974.
[21] V.V. Rondinella, J. Cobos, T. Wiss, D. Staicu, in: Proceedings of the ICEM '05-ASME 2005, Glasgow, UK, 2005, p. 1275.